

Conformational study of 2-arylo-1-vinylpyrroles

Yury Yu. Rusakov,¹ Leonid B. Krivdin,^{1*} Elena Yu. Senotrusova,¹ Elena Yu. Schmidt,¹ Alexander M. Vasiltssov,¹ Albina I. Mikhaleva,¹ Boris A. Trofimov,¹ Oleg A. Dyachenko,² Anatolii N. Chekhlov² and Olga N. Kazheva²

¹ A. E. Favorsky Institute of Chemistry, Irkutsk, Siberian Branch of the Russian Academy of Sciences, Favorsky St. 1, 664033 Irkutsk, Russia

² Institute of Problems of Chemical Physics, Russian Academy of Sciences, Semenov St. 1, 142432 Chernogolovka, Moscow District, Russia

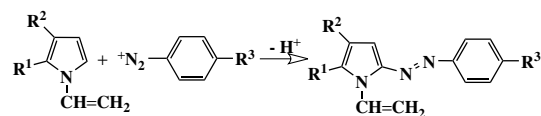
Received 26 September 2006; Revised 24 October 2006; Accepted 26 October 2006

Conformational study of 2-phenylazo-1-vinylpyrrole and 2-(4-bromophenyl)azo-5-methyl-1-vinylpyrrole was performed on the basis of the experimental measurements and high-level *ab initio* calculations of their ¹³C–¹³C and ¹³C–¹H spin–spin coupling constants, showing marked stereochemical behaviour upon the internal rotation of the vinyl group and the pyrrolyl moiety. In liquid phase, both compounds were found to adopt predominant *s-trans-s-trans* conformation with the noticeable population (*ca.* 30%) of the higher-energy *s-cis-s-trans* conformation in the latter compound. As follows from the X-ray data, 2-phenylazo-1-vinylpyrrole crystallizes in *s-trans-s-trans* conformation while the crystalline molecular structure of 2-(4-bromophenyl)azo-5-methyl-1-vinylpyrrole is *s-cis-s-trans*. Copyright © 2006 John Wiley & Sons, Ltd.

KEYWORDS: NMR; ¹³C NMR; X ray; spin–spin coupling constant; lone-pair effect; SOPPA; conformational analysis; 2-arylo-1-vinylpyrroles

INTRODUCTION

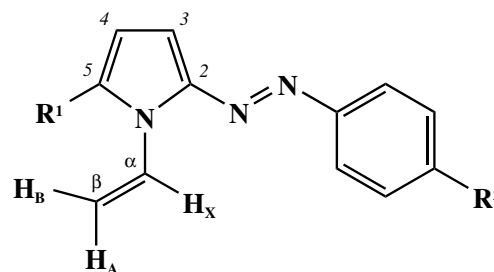
Aryl- and hetarylazopyrrole dyes have been attracting much attention over the past decade owing to their rapidly increasing role in the design of advanced polymer materials and chemical optoelectronic devices possessing conducting and non-linear optical properties.¹ In spite of recent spectacular strides in the chemistry and applications of azopyrrolic dyes, very little is known about their vinyl congeners. Meanwhile, the vinyl substituent could multiply the potential of these compounds, imparting them diverse multi-faceted extra reactivity including polymerizability. A limited but important family of such compounds is the long-known azo coupled bile pigments (serum bilirubin and related species).² As a measure of their importance, the synthesis of bilirubin-based C-vinyl arylazopyrroles helped to elucidate the mechanism of anti-oxidation by bilirubin and its metabolites as well as their important role as anti-oxidants in controlling various oxidative stresses in humans.³ Apart from this rather specific class of arylazo vinylpyrroles, to the best of our knowledge, no similar dyes with vinyl substituent in the pyrrole ring, especially at the nitrogen atom, were known prior to the very recent publication⁴ by some of us reporting the synthesis of a representative series of 2-arylo-1-vinylpyrroles through the azo coupling of the corresponding 1-vinylpyrroles with arenediazonium salts (Scheme 1).



R¹ = H, Alk, Ar, 2-furyl, 2-thienyl; R² = H; R¹, R² = (CH₂)₄; R₃ = H, OAlk, NO₂, Br.

Scheme 1. Synthesis of 2-arylo-1-vinylpyrroles.

In the present communication, a detailed conformational study of the two representative compounds from this series, 2-phenylazo-1-vinylpyrrole (**1**) and 2-(4-bromophenyl)azo-5-methyl-1-vinylpyrrole (**2**), has been performed on the basis of the experimental measurements and high-level *ab initio* calculations of their ¹³C–¹³C and ¹³C–¹H spin–spin coupling constants.

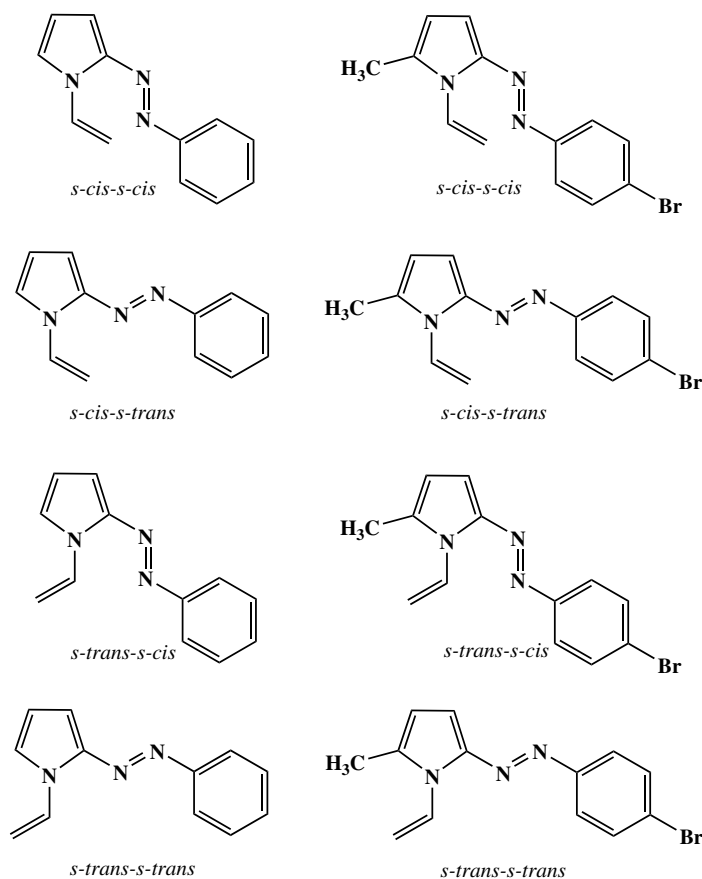


R¹ = R² = H (**1**); R¹ = CH₃, R² = Br (**2**).

*Correspondence to: Leonid B. Krivdin, A. E. Favorsky Institute of Chemistry, Irkutsk, Siberian Branch of the Russian Academy of Sciences, Favorsky St. 1, 664033 Irkutsk, Russia.
E-mail: krivdin_office@irioc.irk.ru

RESULTS AND DISCUSSION

Internal rotation of the vinyl group around the C^α–N bond and that of the pyrrolyl moiety around the C²–N bond



Scheme 2. Possible rotational conformations of 2-phenylazo-1-vinylpyrrole (**1**) and 2-(4-bromophenyl)azo-5-methyl-1-vinylpyrrole (**2**).

in 2-arylo-1-vinylpyrroles result in four possible rotational conformations of **1** and **2**, namely, *s-trans-s-trans*, *s-trans-s-cis*, *s-cis-s-trans*, and *s-cis-s-cis* (Scheme 2). As follows from the present MP2/6-311G* calculations, of the four corresponding conformations, only the former three can be located as true conformers providing no imaginary frequencies (as confirmed by the harmonic vibrational frequency analysis). On the other hand, all attempts to locate the fourth *s-cis-s-cis* conformation as the stationary point on the rotational potential energy surface, for both **1** and **2**, proved to be unsuccessful, resulting in the inevitable *s-cis-s-cis* → *s-cis-s-trans* conversion. Equilibrium structures optimized at the MP2/6-311G* level and relative energies of the three conformers of **1** and **2**, namely, *s-trans-s-trans*, *s-trans-s-cis*, and *s-cis-s-trans*, are shown in Figs 1 and 2 while the located saddle points (transition states in the *s-cis-s-cis* → *s-cis-s-trans* conversion) of both **1** and **2** are presented in Fig. 3.

It is immediately obvious that both compounds, considered as isolated molecules, adopt predominant *s-trans-s-trans* conformation with essential out-of-plane deviations of the vinyl group (*ca.* 25° in **1** and *ca.* 38° in **2**). On the other hand, the second favorable conformer of **1** is *s-trans-s-cis* (1.5 kcal mol⁻¹) while in the case of **2**, it is *s-cis-s-trans* with a much lower relative energy (0.5 kcal mol⁻¹). Accordingly, the highest-energy third conformers of **1** and **2** are respectively, *s-cis-s-trans* (1.8 kcal mol⁻¹) and *s-trans-s-cis* (1.2 kcal mol⁻¹).

As evident from the determined X-ray molecular structures of **1** and **2** (Fig. 4), the azo group in both compounds has *E*-configuration, as expected. In azopyrrole **1**, the –N=N– moiety lies in the plane of the pyrrole and benzene rings (the dihedral angles are 0.0 and 3.5°, respectively). The dihedral angle between the vinyl group plane and the pyrrole ring is 7.1°, with the antiperiplanar orientation to the azo group. Thus, the whole molecule of 2-phenylazo-1-vinylpyrrole (**1**) is essentially planar in crystalline state, providing the maximal conjugation and intra-molecular charge transfer through the four interacting π-systems. In azopyrrole **2**, the dihedral angle between the azo group and the plane of the pyrrole ring is also small, 2.4°. However, the azo group of **2** provides a noticeable out-of-plane deviation with respect to the benzene ring, 7.5°, while the dihedral angle between the planes of the vinyl group and the pyrrole ring in **2** amounts to 20.6°, which is essentially larger than that in **1**. However, what is most interesting is that in the crystalline phase of both compounds the pyrrolyl moiety is *s-trans*, while the N-vinyl group is *s-trans* in **1** and *s-cis* in **2**. This is not so in the isolated molecule of **2** adopting the predominant *s-trans-s-trans* conformation, though with a noticeable population of the second higher-energy *s-cis-s-trans* conformer, as follows from the present MP2/6-311G* calculations (Fig. 2).

It is noteworthy that **1** and **2** show different conformational behaviour as isolated molecules and have different stereochemical molecular structures in crystalline state. It

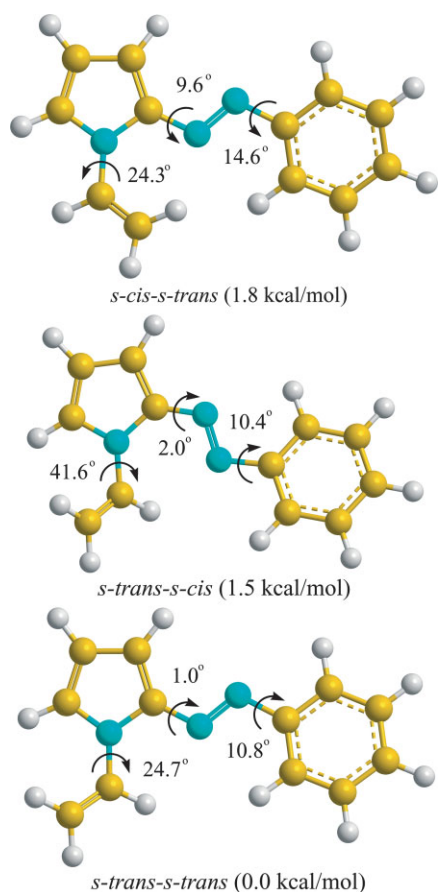


Figure 1. Rotational conformers of 2-phenylazo-1-vinylpyrrole (**1**) optimized at the MP2/6-311G* level (relative energies are given in parentheses). Element colours: carbon, yellow; nitrogen, cyan; hydrogen, grey.

was thus a rewarding goal to perform conformational analysis of **1** and **2** in liquid phase on the basis of the NMR data substantiated by the high-level *ab initio* calculations of spin–spin coupling constants, providing important stereochemical information on their structure.

To study conformational behaviour of **1** and **2**, we performed experimental measurements together with theoretical calculations of $J(\text{C}, \text{C})$ and $J(\text{C}, \text{H})$ spin–spin coupling constants showing marked stereochemical dependence upon the internal rotation around the $\text{C}^\alpha\text{--N}$ and $\text{C}^2\text{--N}$ bonds. Carbon–carbon coupling constants were measured from the INADEQUATE spectra while carbon–hydrogen couplings were measured and unambiguously assigned by the HSQC and HMBC experiments, as illustrated in Figs 5 and 6. The calculations of spin–spin couplings in different conformations of **1** and **2** were performed at the *Second Order Polarization Propagator Approach* (SOPPA)⁵ level taking into account all four coupling contributions, namely, Fermi contact (J_{FC}), spin-dipolar (J_{SD}), diamagnetic spin-orbital (J_{DSO}), and paramagnetic spin-orbital (J_{PSO}). Correlation-consistent basis set, cc-pVDZ,⁶ augmented with two core *s*-functions of Woon and Dunning⁷ on coupled carbons, cc-pVDZ-Cs, was applied, as described elsewhere.⁸ Coupled hydrogens were assigned accordingly with the basis set aug-cc-pVTZ-J of Sauer *et al.*⁹ including four tight *s*-functions and optimized for the calculations of spin–spin coupling constants. Recently, the

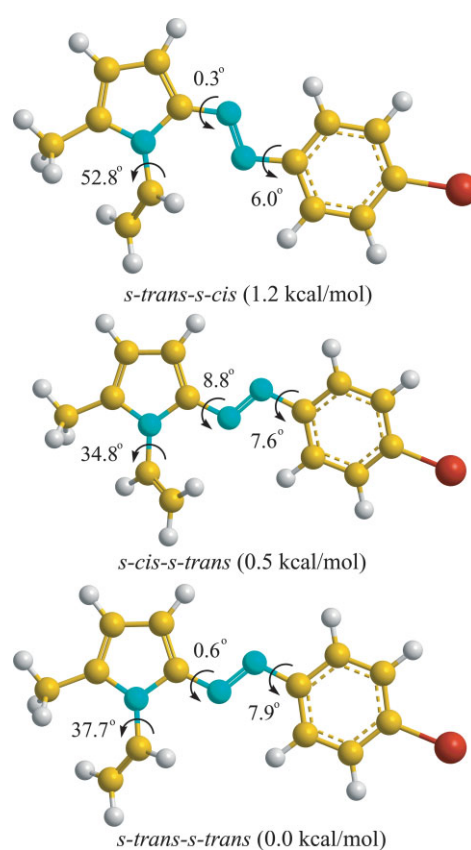


Figure 2. Rotational conformers of 2-(4-bromophenyl)azo-5-methyl-1-vinylpyrrole (**2**) optimized at the MP2/6-311G* level (relative energies are given in parentheses). Element colours: carbon, yellow; nitrogen, cyan; bromine, red; hydrogen, grey.

high-level *ab initio* SOPPA-based calculations of $J(\text{C}, \text{C})$ and $J(\text{C}, \text{H})$ spin–spin couplings in a number of organic molecules including polycycloalkanes,¹⁰ azomethines,¹¹ five- and six-membered heterocycles,¹² and other compounds^{13,14} demonstrated their high reliability and growing perspectives in stereochemical studies, which encouraged us to use SOPPA in the present paper.

Calculated $J(\text{C}, \text{C})$ and $J(\text{C}, \text{H})$ couplings in *s-trans-s-trans*, *s-trans-s-cis*, and *s-cis-s-trans* conformers of **1** and **2** together with their experimental values measured in CDCl_3 solutions are presented in Table 1. It follows that calculated total values of all couplings in *s-trans-s-trans* conformer of both compounds are in very good agreement with the experiment. The FC contribution dominates in all cases; however, the non-contact PSO contribution dramatically improves this agreement in the case of all $^1J(\text{C}, \text{C})$ couplings, and hence it should be taken into account without fail.

It is noteworthy that this agreement goes from bad to worse when taking into consideration the other two conformers, *s-trans-s-cis* and *s-cis-s-trans*. Indeed, this is clearly seen when comparing the most critical couplings showing marked stereochemical dependence in the different conformations of **1** and **2**. For example: $^1J(\text{C-2}, \text{C-3}) = 72.05$ Hz in *s-trans-s-trans* while it is 76.88 Hz in *s-trans-s-cis* conformations of **1** (exptl: 72.8 Hz); $^1J(\text{C}_\alpha, \text{H}_X) = 182.08$ Hz in *s-trans-s-trans* while it is 174.46 Hz in *s-cis-s-trans* and 188.78 Hz in *s-trans-s-cis* conformations of **1**

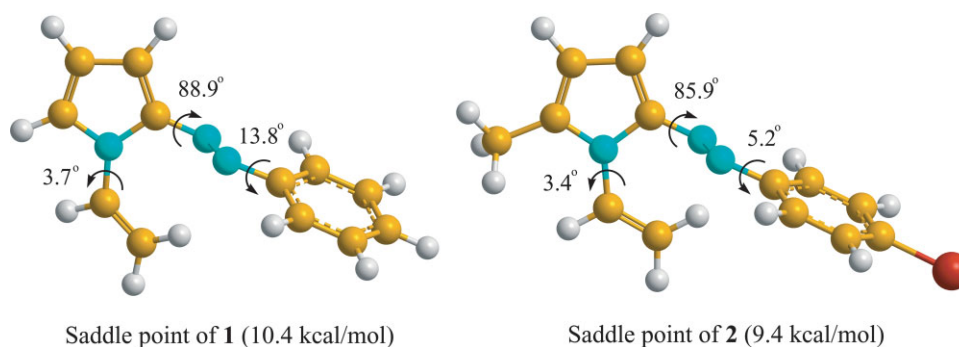


Figure 3. Saddle points (transition states in the *s-cis-s-cis* → *s-cis-s-trans* conversion) of 2-phenylazo-1-vinylpyrrole (**1**) and 2-(4-bromophenyl)azo-5-methyl-1-vinylpyrrole (**2**) located at the MP2/6-311G* level using the Newton–Rafson method (relative energies with respect to the corresponding lowest-energy predominant conformations of **1** and **2** are given in parentheses). Element colours: carbon, yellow; nitrogen, cyan; bromine, red; hydrogen, grey.

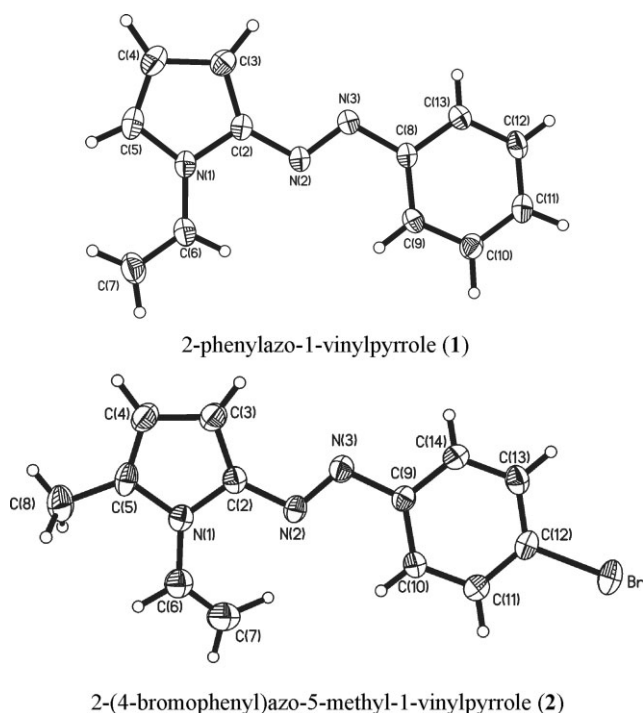


Figure 4. ORTEP diagrams of the X-ray molecular structures of 2-phenylazo-1-vinylpyrrole (**1**) and 2-(4-bromophenyl)azo-5-methyl-1-vinylpyrrole (**2**).

(exptl: 183.1 Hz); $^1J(C_\beta, H_A) = 163.05$ Hz in *s-trans-s-trans* while it is 159.36 Hz in *s-cis-s-trans* conformations of **1** (exptl: 164.1 Hz); $^1J(C_\beta, H_B) = 158.53$ Hz in *s-trans-s-trans* while it is 167.04 Hz in *s-cis-s-trans* conformations of **1** (exptl: 157.2 Hz); $^3J(C-2, H_X) = 0.71$ Hz in *s-trans-s-trans* while it is 4.59 Hz in *s-cis-s-trans* conformations of **1** (exp: 1.1 Hz), and so on. In much the same way, analogous convincing examples could be presented for the second azopyrrole **2**.

Apparently, these results indicate that both compounds, **1** and **2**, adopt a predominant *s-trans-s-trans* conformation, and also that this unambiguously follows from the analysis of the dihedral angle dependences of the most characteristic $J(C, C)$ and $J(C, H)$ couplings in the model structure **1** presented in Figs 7–9. It appears that spin–spin couplings $^1J(C-2, C-3)$, and, on the other hand, $^3J(C-2, H_X)$ and $^3J(C-5, H_X)$, display

the most straightforward and understandable dihedral angle dependences with respect to the internal rotations around the $C^\alpha-N$ and C^2-N bonds.

Indeed, $^1J(C-2, C-3)$ increases by *ca.* 10 Hz when rotating the pyrrolyl moiety around the C^2-N bond while going from *s-trans-s-trans* ($\varphi = 0^\circ$) to *s-trans-s-cis* ($\varphi = 180^\circ$) conformation, Fig. 7. The increase of $^1J(C-2, C-3)$ in the region of $\Delta\varphi = 0-90^\circ$ is due to the decrease of the negative azo nitrogen lone-pair contribution while further increase of $^1J(C-2, C-3)$ in the range of $\Delta\varphi = 90-180^\circ$ should be ascribed to the increase of the positive nitrogen lone-pair contribution to this coupling. The nature of this interesting effect, providing the marked difference between $^1J(C-2, C-3)$ in *s-trans-s-trans* and *s-trans-s-cis* conformations of **1** and **2**, could be accounted for by the three different contributions, namely, those of (i) the nitrogen lone-pair, (ii) the carbon–carbon bonds containing coupling carbons, and (iii) the carbon inner core orbitals. The first one relates to the direct azo nitrogen lone-pair participation in the transmission of spin–spin coupling giving a positive contribution to $^1J(C-2, C-3)$ in *s-trans-s-cis* and a negative one in *s-trans-s-trans* conformations (primary lone-pair effect), as was found by Barone *et al.*¹⁵ who performed the dissection of $^1J(C, C)$ in acetoxime into orbital contributions involving those of the nitrogen lone-pair by applying the *Natural J Coupling* (NJC) scheme¹⁶ based on the *Natural Localized Molecular Orbitals* (NLMO) analysis of Reed and Weinhold.¹⁷ On the other hand, the second and the third contributions originate mainly in the charge transfer from the nitrogen lone-pair to the antibonding orbital of the adjacent carbon–carbon (or carbon–hydrogen) bond in *trans* orientation to the nitrogen lone-pair, as explained in detail by Cuevas and Juaristi.¹⁸ This charge transfer interaction, very similar to anomeric effect, results in the substantial lengthening of the *transoid* carbon–carbon bond and hence in the negative contribution to $^1J(C-2, C-3)$ in *s-trans-s-trans* conformer (secondary lone-pair effect).

It is the cooperation of these different intra-molecular interactions that results in a dramatic difference of *ca.* 10 Hz between $^1J(C-2, C-3)$ in *s-trans-s-trans* and *s-trans-s-cis* conformations of **1** and **2**. Comparison of the measured values of $^1J(C-2, C-3) = 72.8$ Hz in **1** and 71.6 Hz in **2** with those displayed in Fig. 7 suggests that in both compounds

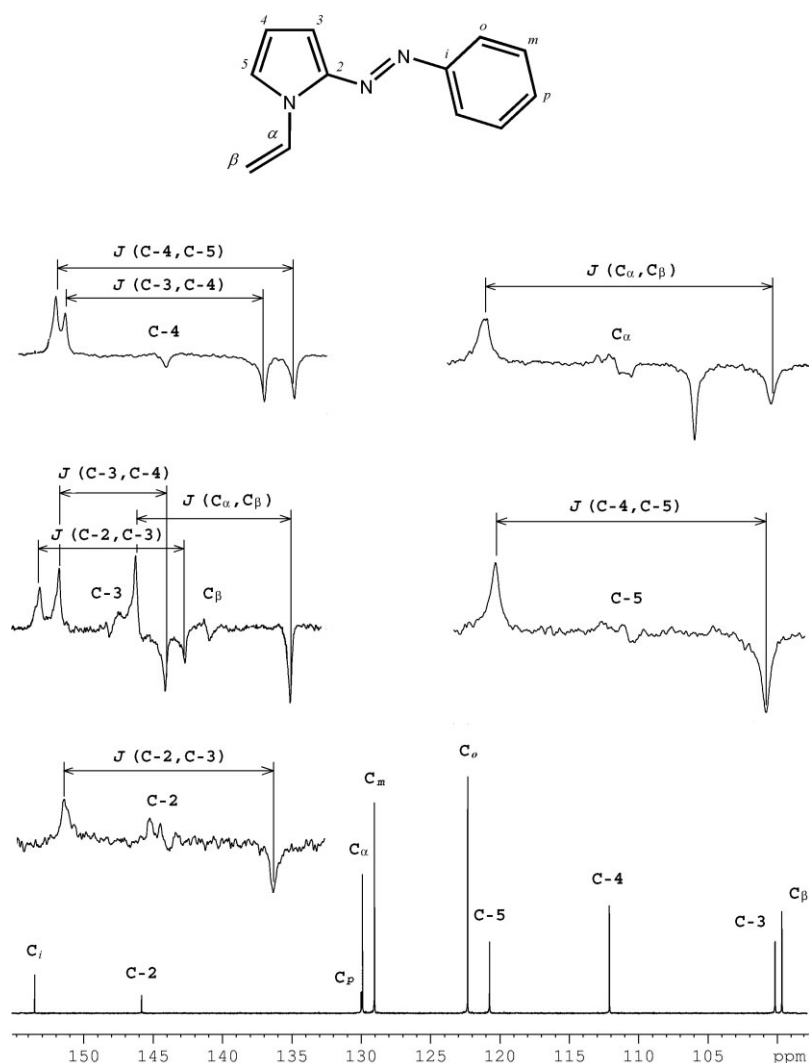


Figure 5. INADEQUATE ^{13}C NMR spectrum of 2-phenylazo-1-vinylpyrrole (**1**) in CDCl_3 (101.61 MHz).

the pyrrolyl moiety is in *s-trans* orientation to the azo group. Indeed, according to Fig. 7, this coupling is *ca* 73 Hz for the *s-trans* orientation of the azo group in *s-trans-s-trans* conformation while it is *ca*. 83 Hz (~ 10 Hz larger!) for the opposite *s-trans-s-cis* conformation.

On the other hand, $^3J(\text{C-2}, \text{H}_X)$ and $^3J(\text{C-5}, \text{H}_X)$ couplings demonstrate classical Karplus-type dihedral angle dependence with respect to the internal rotation of the vinyl group around the $\text{C}_\alpha\text{-N}$ bond (Fig. 8), which can be expanded into the Fourier series, Eqns (1) and (2):

$$^3J(\text{C-2}, \text{H}_X) = 1.92 - 2.15 \cos \varphi + 1.36 \cos 2\varphi \quad (1)$$

$$^3J(\text{C-5}, \text{H}_X) = 2.27 + 0.69 \cos \varphi + 1.46 \cos 2\varphi \quad (2)$$

Again, comparison of the respective experimental values of $^3J(\text{C-2}, \text{H}_X)$ and $^3J(\text{C-5}, \text{H}_X)$ given in Table 1 with the former theoretical results suggests that in both compounds the orientation of the vinyl group is essentially *s-trans*. This assertion is substantiated by the dependence of the dihedral angle of the three one-bond carbon–hydrogen couplings of the vinyl group, $^1J(\text{C}_\alpha, \text{H}_X)$, $^1J(\text{C}_\beta, \text{H}_A)$, and $^1J(\text{C}_\beta, \text{H}_B)$, depicted in Fig. 9, in comparison with the corresponding experimental data (Table 1). The latter three couplings also

provide a marked dihedral angle dependence with respect to the internal rotation of the vinyl group around the $\text{C}_\alpha\text{-N}$ bond following the respective changes in the *s*-characters of the corresponding C–H bonds.

Finally, we estimated the conformational ratios of both azopyrroles in liquid phase (solutions in CDCl_3) on the basis of the statistical treatment of the calculated model dihedral angle dependences presented in Figs 7–9 and expanded into the Fourier series by φ in comparison with the corresponding experimental values of $J(\text{C}, \text{C})$ and $J(\text{C}, \text{H})$ couplings given in Table 1. The results are as follows: 2-phenylazo-1-vinylpyrrole (**1**) exists almost entirely as the *s-trans-s-trans* conformer with the $\sim 10\%$ population of the higher-energy *s-cis-s-trans* conformer while 2-(4-bromophenyl)azo-5-methyl-1-vinylpyrrole (**2**) provides a *ca* 70:30 mixture of *s-trans-s-trans* and *s-cis-s-trans* conformations. This finding is substantiated by the pure theoretical energy-based conformational analysis of both azopyrroles (Fig. 10). According to these data, 2-phenylazo-1-vinylpyrrole (**1**) and 2-(4-bromophenyl)azo-5-methyl-1-vinylpyrrole (**2**) exist in the equilibrium mixture of *s-trans-s-trans* and *s-cis-s-trans* conformations in the ratios of 96:4 and 69:31, which is in very good agreement with the

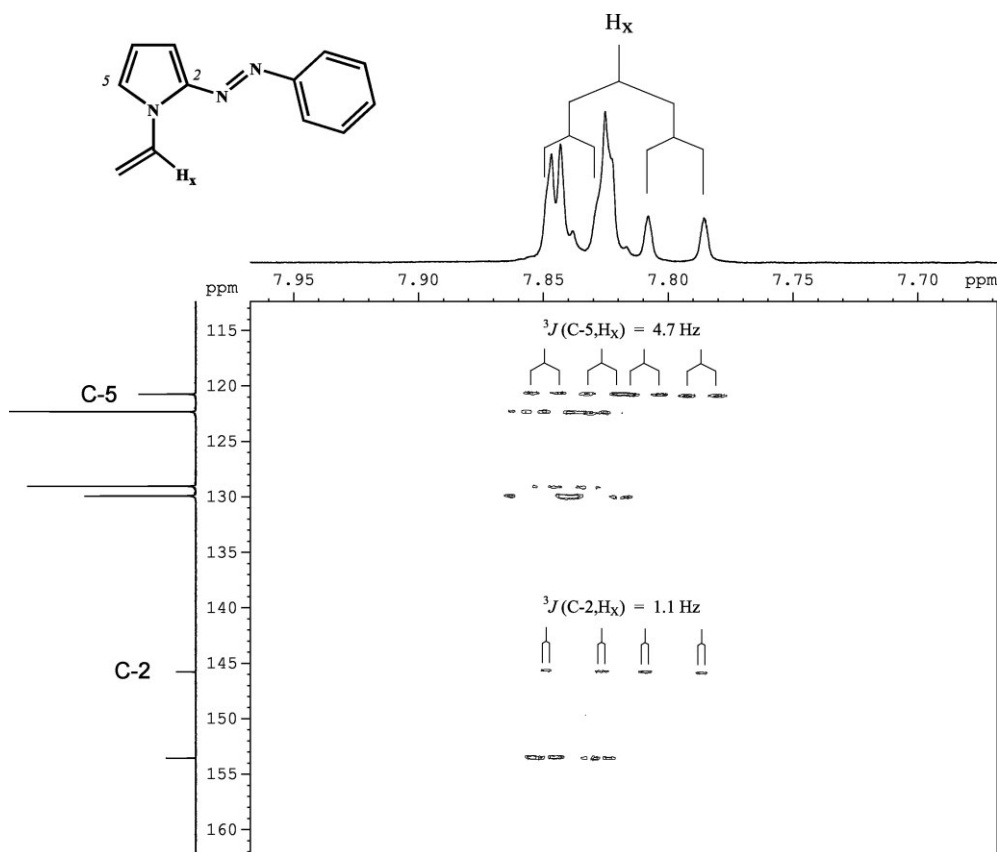


Figure 6. $^{13}\text{C}/^1\text{H}$ HMBC contour plot of 2-phenylazo-1-vinylpyrrole (**1**) in CDCl_3 used to assign $^3J(\text{C}-2, \text{H}_x)$ and $^3J(\text{C}-5, \text{H}_x)$.

corresponding results derived from the $J(\text{C}, \text{C})$ and $J(\text{C}, \text{H})$ experimental data.

s-trans-s-trans conformation while in contrast the crystalline molecular structure of **2** is *s-cis-s-trans*.

CONCLUDING REMARKS

2-Phenylazo-1-vinylpyrrole (**1**) and 2-(4-bromophenyl)azo-5-methyl-1-vinylpyrrole (**2**), the representative members of the 2-arylo-1-vinylpyrroles series, show different conformational behaviour as isolated molecules and in solution and have different stereochemical molecular structures in crystalline state. Both compounds, considered as isolated molecules, adopt a predominant *s-trans-s-trans* conformation with essential out-of-plane deviations of the vinyl group (*ca* 25° in **1** and *ca* 38° in **2**). On the other hand, the second favorable conformer of **1** is *s-trans-s-cis* (1.5 kcal mol⁻¹) while in the case of **2**, it is *s-cis-s-trans* with a much lower relative energy (0.5 kcal mol⁻¹). Accordingly, the highest-energy third conformers of **1** and **2** are, respectively, *s-cis-s-trans* (1.8 kcal mol⁻¹) and *s-trans-s-cis* (1.2 kcal mol⁻¹). In liquid phase, both compounds adopt predominant *s-trans-s-trans* conformation with considerable population (*ca* 30%) of the second *s-cis-s-trans* conformation in **2**, as follows from the experimental measurements together with theoretical calculations of $J(\text{C}, \text{C})$ and $J(\text{C}, \text{H})$ spin-spin coupling constants providing marked stereochemical dependences upon the internal rotation around the C^α-N and C²-N bonds in 2-arylo-1-vinylpyrroles. This result is in line with the pure theoretical energy-based conformational analysis of both azopyrroles. On the basis of the X-ray data, **1** crystallizes in

EXPERIMENTAL

NMR measurements

^{13}C NMR spectra were recorded on a Bruker AVANCE 400 MHz spectrometer in a 10-mm broadband probe at 300 K in CDCl_3 with hexamethyldisiloxane as an internal standard. Carbon-carbon coupling constants were measured from the natural-abundance ^{13}C NMR spectra (101.61 MHz) using the INADEQUATE pulse sequence of Bax *et al.*¹⁹ adjusted for $J = 70$ Hz. Settings for the INADEQUATE experiments were as follows: 90° pulse length, 12–14 μs; spectral width, 10–15 kHz; acquisition time, 4–6 s; relaxation delay, 6–10 s; characteristic delay $\tau = 1/4J$, 3.6 ms; digital resolution 0.05–0.1 Hz per pt; accumulation time, 12 h. One-bond carbon-hydrogen coupling constants were measured from the proton-coupled ^{13}C NMR spectra (101.61 MHz) using the same spectral widths, acquisition times, relaxation delays, and digital resolutions as in the INADEQUATE experiments, and their assignment was confirmed by the $^{13}\text{C}/^1\text{H}$ HSQC spectra. Vicinal carbon-hydrogen coupling constants were measured from the $^{13}\text{C}/^1\text{H}$ HMBC spectra acquired with 64×8 k complex points in t_1 and t_2 for spectral widths of 5000 Hz in t_1 (^{13}C) and 500 Hz in t_2 (^1H) using the following settings: acquisition time, 4 s; relaxation delay, 6 s; digital resolution, 0.1 Hz per pt in F1 (^{13}C) and 0.05 Hz in F2 (^1H); total acquisition time, 4 h.

Table 1. Spin-spin coupling constants $^{13}\text{C}-^{13}\text{C}$ and $^{13}\text{C}-^1\text{H}$ of **1** and **2** calculated at the SOPPA level in comparison with experimental values^a

Cmpd.	Conformer	Coupling constant	J_{DSO}	J_{PSO}	J_{SD}	J_{FC}	J	Exp.	
1	<i>s-trans-s-trans</i>	$^1J(\text{C-2, C-3})$	0.32	-6.03	1.72	76.04	72.05	72.8	
		$^1J(\text{C-3, C-4})$	0.24	-4.97	0.78	63.40	59.45	- ^b	
		$^1J(\text{C-4, C-5})$	0.25	-6.14	1.42	69.78	65.31	64.1	
		$^1J(\text{C}_\alpha, \text{C}_\beta)$	0.17	-8.20	3.33	83.75	79.05	77.6	
		$^1J(\text{C}_\alpha, \text{H}_X)$	0.97	-0.11	0.22	181.00	182.08	183.1	
		$^1J(\text{C}_\beta, \text{H}_A)$	0.56	0.43	0.22	161.84	163.05	164.1	
		$^1J(\text{C}_\beta, \text{H}_B)$	0.63	0.41	0.22	157.27	158.53	157.2	
		$^3J(\text{C-2, H}_X)$	0.15	-0.25	0.00	0.81	0.71	1.1	
		$^3J(\text{C-5, H}_X)$	-0.47	0.22	0.00	4.53	4.28	4.7	
	<i>s-cis-s-trans</i>	$^1J(\text{C-2, C-3})$	0.32	-6.08	1.71	75.76	71.71		
		$^1J(\text{C-3, C-4})$	0.24	-4.97	0.78	63.21	59.26		
		$^1J(\text{C-4, C-5})$	0.25	-6.12	1.41	69.86	65.4		
		$^1J(\text{C}_\alpha, \text{C}_\beta)$	0.18	-8.23	3.39	84.03	79.37		
		$^1J(\text{C}_\alpha, \text{H}_X)$	0.95	0.05	0.13	173.33	174.46		
		$^1J(\text{C}_\beta, \text{H}_A)$	0.58	0.40	0.20	158.18	159.36		
		$^1J(\text{C}_\beta, \text{H}_B)$	0.66	0.17	0.29	165.92	167.04		
		$^3J(\text{C-2, H}_X)$	-0.40	0.18	-0.01	4.82	4.59		
		$^3J(\text{C-5, H}_X)$	0.14	-0.22	0.01	3.03	2.96		
	<i>s-trans-s-cis</i>	$^1J(\text{C-2, C-3})$	0.31	-6.02	1.54	81.05	76.88		
		$^1J(\text{C-3, C-4})$	0.24	-4.92	0.75	63.51	59.58		
		$^1J(\text{C-4, C-5})$	0.25	-6.20	1.41	68.95	64.41		
		$^1J(\text{C}_\alpha, \text{C}_\beta)$	0.18	-8.36	3.36	82.83	78.01		
		$^1J(\text{C}_\alpha, \text{H}_X)$	0.98	-0.21	0.29	187.72	188.78		
		$^1J(\text{C}_\beta, \text{H}_A)$	0.57	0.38	0.22	160.57	161.74		
		$^1J(\text{C}_\beta, \text{H}_B)$	0.64	0.34	0.22	157.86	159.06		
		$^3J(\text{C-2, H}_X)$	0.07	-0.15	0.02	-0.22	-0.28		
		$^3J(\text{C-5, H}_X)$	-0.40	0.19	-0.05	3.84	3.58		
	2	<i>s-trans-s-trans</i>	$^1J(\text{C-2, C-3})$	0.33	-5.98	1.70	75.07	71.12	71.6
			$^1J(\text{C-3, C-4})$	0.25	-4.98	0.74	63.18	59.19	- ^b
			$^1J(\text{C-4, C-5})$	0.29	-6.20	1.33	69.64	65.06	64.4
			$^1J(\text{C}_\alpha, \text{C}_\beta)$	0.19	-8.31	3.27	82.55	77.7	77.3
			$^1J(\text{C}_\alpha, \text{H}_X)$	1.00	-0.12	0.23	180.39	181.5	178.7
			$^1J(\text{C}_\beta, \text{H}_A)$	0.59	0.36	0.22	159.91	161.08	160.9
$^1J(\text{C}_\beta, \text{H}_B)$			0.68	0.27	0.24	158.37	159.56	160.9	
$^3J(\text{C-2, H}_X)$			0.16	-0.24	0.00	0.63	0.55	2.3	
$^3J(\text{C-5, H}_X)$			-0.38	0.17	-0.01	4.47	4.25	3.9	
<i>s-cis-s-trans</i>		$^1J(\text{C-2, C-3})$	0.33	-6.08	1.70	74.82	70.77		
		$^1J(\text{C-3, C-4})$	0.25	-5.02	0.71	63.29	59.23		
		$^1J(\text{C-4, C-5})$	0.29	-6.19	1.33	69.58	65.01		
		$^1J(\text{C}_\alpha, \text{C}_\beta)$	0.18	-8.42	3.32	83.04	78.12		
		$^1J(\text{C}_\alpha, \text{H}_X)$	1.02	0.01	0.25	173.77	175.05		
		$^1J(\text{C}_\beta, \text{H}_A)$	0.59	0.32	0.22	158.16	159.29		
		$^1J(\text{C}_\beta, \text{H}_B)$	0.68	0.11	0.23	164.63	165.65		
		$^3J(\text{C-2, H}_X)$	-0.36	0.17	-0.01	4.12	3.92		
		$^3J(\text{C-5, H}_X)$	0.14	-0.22	0.01	1.87	1.80		
<i>s-trans-s-cis</i>		$^1J(\text{C-2, C-3})$	0.32	-5.98	1.52	80.05	75.91		
		$^1J(\text{C-3, C-4})$	0.25	-4.92	0.72	63.13	59.18		
		$^1J(\text{C-4, C-5})$	0.29	-6.25	1.33	69.25	64.62		
		$^1J(\text{C}_\alpha, \text{C}_\beta)$	0.29	-6.25	1.33	69.25	64.62		
		$^1J(\text{C}_\alpha, \text{H}_X)$	0.19	-8.48	3.39	82.87	77.97		
		$^1J(\text{C}_\beta, \text{H}_A)$	1.02	-0.21	0.28	186.55	187.64		
		$^1J(\text{C}_\beta, \text{H}_B)$	0.60	0.32	0.22	159.40	160.54		
		$^3J(\text{C-2, H}_X)$	0.69	0.25	0.22	157.83	158.99		
		$^3J(\text{C-5, H}_X)$	0.09	-0.13	0.02	-0.24	-0.26		
			-0.30	0.13	-0.04	3.54	3.33		

^a All couplings and coupling contributions are in Hz.^b Not measured owing to signal overlapping.

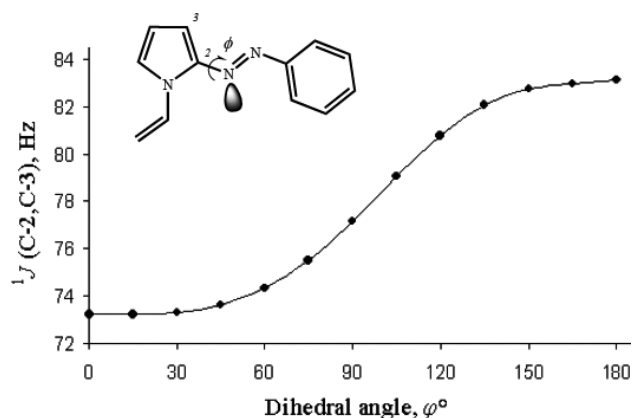


Figure 7. Dihedral angle dependence of $^1J(\text{C-2}, \text{C-3})$ in 2-phenylazo-1-vinylpyrrole (**1**) calculated at the SOPPA level.

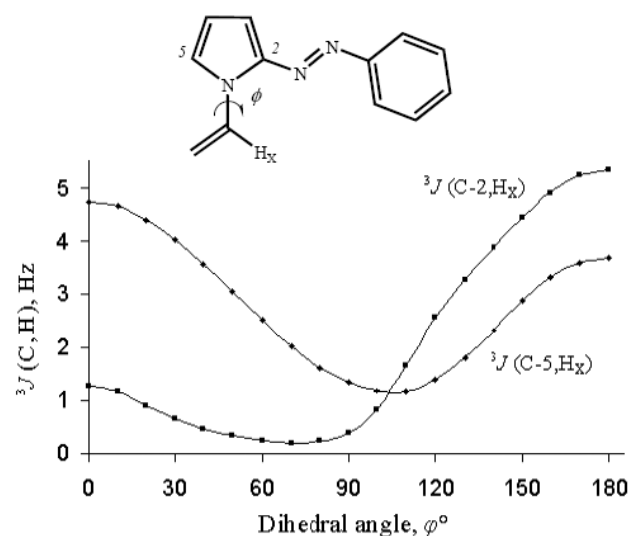


Figure 8. Dihedral angle dependences of $^3J(\text{C-2}, \text{H}_X)$ and $^3J(\text{C-5}, \text{H}_X)$ in 2-phenylazo-1-vinylpyrrole (**1**) calculated at the SOPPA level.

Computational details

Geometric optimizations were performed with the GAMESS code,²⁰ at the MP2 level,²¹ using the 6-311G* basis set of Pople and coworkers²² without symmetry constraints, i.e. assuming the C_1 symmetry point group. Calculations of spin–spin coupling constants have been carried out using the DALTON package²³ at the SOPPA level⁵ with the correlation-consistent basis sets of Dunning and coworkers^{6,7} and Sauer *et al.*,⁹ either taken from the Dalton Basis Sets Library²³ without modifications or slightly modified by adding or removing polarization, core, and tight or diffuse functions, as specified elsewhere.⁸ The SOPPA calculations of $^1J(\text{C}, \text{C})$ and $^1J(\text{C}, \text{H})$ were performed within the C_1 point group as well, and all compounds were adopted in their equilibrium conformations located at the MP2/6-311G* level.

X-ray experiments

The X-ray diffraction data were collected on an Enraf-Nonius CAD-4 diffractometer with graphite-monochromatized $\text{MoK}\alpha$ radiation at room temperature ($\omega 2\theta^{-1}$ -scanning). Crystalline structures were solved by direct methods and Fourier

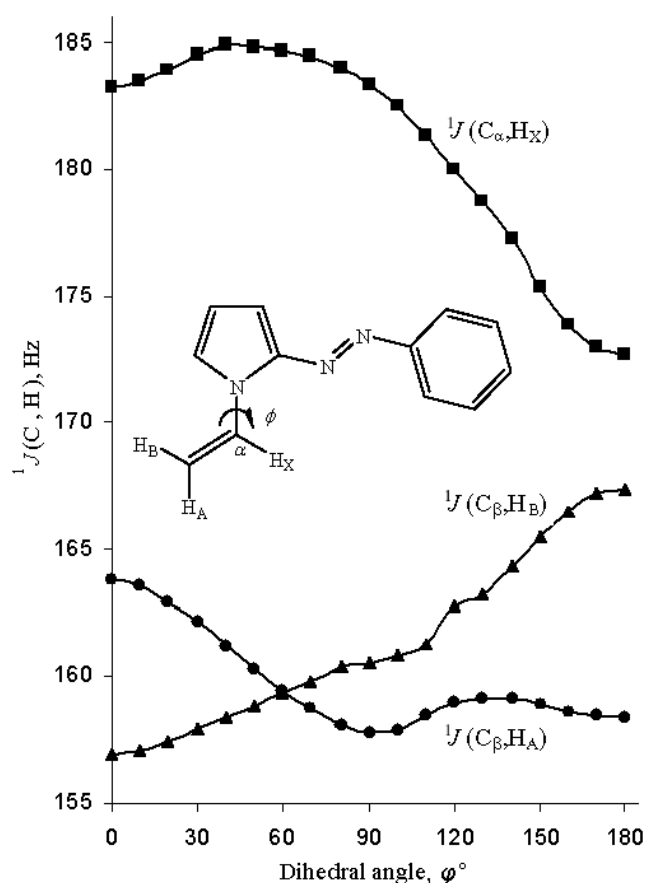


Figure 9. Dihedral angle dependences of $^1J(\text{C}_\alpha, \text{H}_X)$, $^1J(\text{C}_\beta, \text{H}_A)$, and $^1J(\text{C}_\beta, \text{H}_B)$ in 2-phenylazo-1-vinylpyrrole (**1**) calculated at the SOPPA level.

synthesis, the non-hydrogen atoms were refined anisotropically by the full-matrix procedure on F^2 using the SHELXL-97 package.²⁴ Hydrogen atoms were found experimentally and refined isotropically.

Synthesis

Both azopyrroles, **1** and **2**, were prepared according to the following general procedure. To a 0 °C solution of aromatic amine (10 mmol) and aqueous HCl (3 ml) in water (15 ml), a 0 °C solution of NaNO_2 (0.69 g, 10 mmol) in water (10 ml) was added and the mixture was stirred at 0 °C for 0.5 h. The resulting diazonium salt solution was neutralized (pH ~7) with dry NaHCO_3 (3.0 g, 36 mmol). After stirring for 10 min, the solution obtained was poured into a 0 °C solution of 1-vinylpyrrole (10 mmol) in ethanol (10 ml). The mixture was stirred at 0 °C for 2 h. The precipitate was filtered off and dried *in vacuo*. In cases when the solid did not precipitate, the reaction mixture was extracted with Et_2O (15 × 3 ml). The extract was dried with K_2CO_3 and distilled off. The products were purified by column chromatography (Al_2O_3 , eluent – *n*-hexane) or recrystallization from *n*-hexane. Upon storage of the azo coupling products, **1** and **2**, at ambient temperature for several months, neither changes in their UV/vis spectra nor appearance of redundant signals in their ^1H NMR spectra were observed, which evidences their stability.

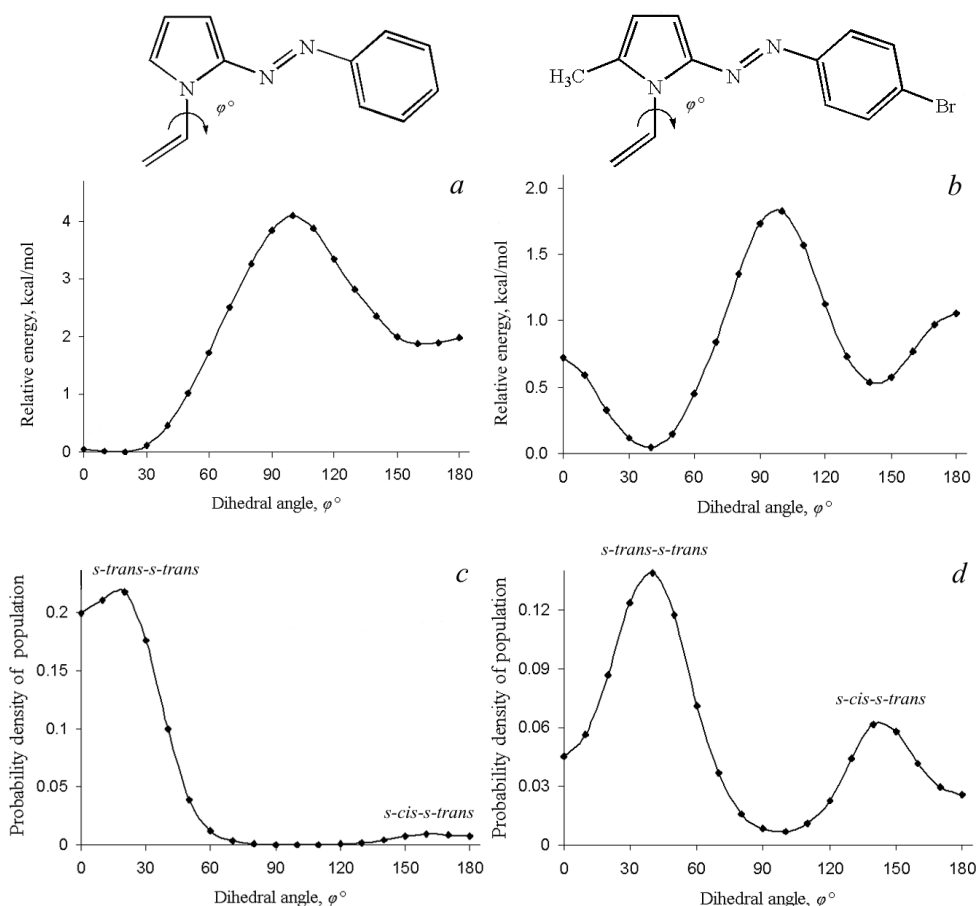


Figure 10. Dihedral angle dependence of the relative energies (a), (b) and statistical distribution of the rotational conformations (c), (d) of **1** and **2** calculated at the MP2/6-311G* level.

2-Phenylazo-1-vinylpyrrole (**1**)

Crimson crystals, mp 72–74 °C. ^1H NMR (CDCl_3) δ : 7.88 (m, 2H, H_o), 7.87 (dd, 1H, H_x , $^3J_{\text{B-X}}$ 16.0 Hz, $^3J_{\text{A-X}}$ 8.8 Hz), 7.52 (m, 2H, H_m), 7.43 (m, 1H, H_p), 7.36 (m, 1H, H_5), 6.79 (m, 1H, H_3), 6.45 (m, 1H, H_4), 5.38 (d, 1H, H_B), 4.97 (d, 1H, H_A). ^{13}C NMR (CDCl_3) δ : 153.46 (C_i), 145.73 (C-2), 129.97 (C_p), 129.84 (C_α), 129.07 (C_m), 122.33 (C_o), 120.73 (C-5), 112.14 (C-4), 100.03 (C-3), 99.66 (C_β). IR (KBr, ν_{max} cm^{-1}): 3165–3105, 1630, 1535, 1501, 1475, 1450, 1410, 1360, 1345, 1305, 1280, 1230, 1180, 1125, 1045, 1005, 955, 905, 880, 800, 765, 710, 675, 650, 580, 550, 500, 450. Calcd (%): C, 73.07; H, 5.62; N 21.30. Found (%): C, 73.24; H, 5.70; N 21.17. $\text{C}_{12}\text{H}_{11}\text{N}_3$.

2-(4-Bromophenyl)azo-5-methyl-1-vinylpyrrole (**2**)

Orange needles, mp 72–74 °C. ^1H NMR (CDCl_3) δ : 7.62 (d, 2H, H_o , $^3J_{o-m}$ 8.8 Hz), 7.53 (d, 2H, H_m), 7.31 (dd, 1H, H_x , $^3J_{\text{B-X}}$ 16.1 Hz, $^3J_{\text{A-X}}$ 9.3 Hz), 6.71 (d, 1H, H_3 , $^3J_{3-4}$ 3.9 Hz), 6.13 (d, 1H, H_4), 5.40 (d, 1H, H_B), 5.16 (d, 1H, H_A), 2.41 (s, 3H, Me). ^{13}C NMR (CDCl_3) δ : 152.57 (C_i), 147.01 (C-2), 135.53 (C-5), 132.16 (C_m), 129.55 (C_α), 123.58 (C_o), 123.01 (C_p), 112.09 (C-4), 108.17 (C_β), 100.93 (C-3), 14.55 (Me). IR (KBr, ν_{max} cm^{-1}): 3127, 3055, 2911, 1643, 1582, 1567, 1535, 1474, 1433, 1416, 1388, 1344, 1303, 1293, 1206, 1182, 1150, 1062, 1026, 1004, 960, 886, 831, 812, 783, 774, 762, 706, 510, 492, 458. Calcd (%): C, 53.81; H, 4.17; Br, 27.54; N 14.48. Found (%): C, 53.97; H, 4.09; Br, 27.51; N 14.33. $\text{C}_{13}\text{H}_{12}\text{BrN}_3$.

Acknowledgements

Financial support from Russian Foundation for Basic Research (Grant No. 05-03-32231) is acknowledged.

REFERENCES

- (a) Yokomichi N, Seki K, Tada S, Yamabe T. *Synth. Met.* 1995; **69**: 577; (b) Zotti G, Zecchin S, Schiavon G, Berlin A, Pagani GA, Canavesi A, Casalbore-Miceli G. *Synth. Met.* 1996; **78**: 51; (c) Chyla A, Kucharski S, Sworakowski J, Bieřkovski M. *Thin Solid Films* 1996; **284–285**: 496; (d) Nero JD, Laks D. *Synth. Met.* 1999; **101**: 440; (e) Zhu Z, Wang Y, Lu Y. *Macromolecules* 2003; **36**: 9585; (f) Wagner-Wysiecka E, Luboch E, Kowalczyk M, Biernat JF. *Tetrahedron* 2003; **59**: 4415; (g) Facchetti A, Abbotti A, Beverina L, van der Boom ME, Dutta P, Evmenenko G, Marks TJ, Pagani GA. *Chem. Mater.* 2002; **14**: 4996; (h) Wang Y, Ma J, Jiang Y. *J. Phys. Chem. A* 2005; **109**: 7197.
- Heirwegh KPM, van Hees GP, Leroy P, van Roy FP, Jansen FH. *Biochem. J.* 1970; **120**: 877.
- Yamaguchi T, Shhiji I, Sugimoto A, Komoda Y, Nakajima H. *Biochim. Biophys. Acta* 1996; **1289**: 110.
- Trofimov BA, Schmidt EYu, Mikhaleva AI, Vasil'tsov AM, Zaitsev AB, Smolyanina NS, Senotrusova EYu, Afonin AV, Ushakov IA, Petrusenko KB, Kazheva ON, Dyachenko OA, Smirnov VV, Schmidt AF, Markova MV, Morozova LV. *Eur. J. Org. Chem.* 2006; **17**: 4021.
- (a) Nielsen ES, Jørgensen P, Oddershede J. *J. Chem. Phys.* 1980; **73**: 6238; (b) Packer MJ, Dalskov EK, Enevoldsen T, Jensen HJA, Oddershede J. *J. Chem. Phys.* 1996; **105**: 5886; (c) Bak KL, Koch H, Oddershede J, Christiansen O, Sauer SPA. *J. Chem. Phys.* 2000; **112**: 4173.

6. (a) Dunning TH Jr. *J. Chem. Phys.* 1989; **90**: 1007; (b) Kendall RA, Dunning TH Jr, Harrison RJ. *J. Chem. Phys.* 1992; **96**: 6796; (c) Woon DE, Dunning TH Jr. *J. Chem. Phys.* 1993; **98**: 1358.
7. Woon DE, Dunning TH Jr. *J. Chem. Phys.* 1995; **103**: 4572.
8. (a) Krivdin LB, Sauer SPA, Peralta JE, Contreras RH. *Magn. Reson. Chem.* 2002; **40**: 187; (b) Sauer SPA, Krivdin LB. *Magn. Reson. Chem.* 2004; **42**: 671; (c) Krivdin LB. *Magn. Reson. Chem.* 2004; **42**: S168; (d) Krivdin LB. *Magn. Reson. Chem.* 2005; **43**: 101.
9. Provasi PF, Aucar GA, Sauer SPA. *J. Chem. Phys.* 2001; **115**: 1324.
10. Krivdin LB. *Magn. Reson. Chem.* 2005; **43**: 101.
11. (a) Krivdin LB, Scherbina NA, Istomina NV. *Magn. Reson. Chem.* 2005; **43**: 435; (b) Scherbina NA, Istomina NV, Krivdin LB. *Russ. J. Org. Chem.* 2005; **41**: 1103; (c) Krivdin LB, Larina LI, Chernyshev KA, Rozentsveig IB. *Magn. Reson. Chem.* 2005; **43**: 937; (d) Krivdin LB, Nedolya NA. *Tetrahedron Lett.* 2005; **46**: 7367; (e) Krivdin LB, Larina LI, Chernyshev KA, Rulev AYU. *Magn. Reson. Chem.* 2006; **44**: 178; (f) Krivdin LB, Larina LI, Chernyshev KA, Keiko NA. *Aust. J. Chem.* 2006; **59**: 211.
12. Rusakov YuYu, Krivdin LB, Schmidt EYu, Mikhaleva AI, Trofimov BA. *Magn. Reson. Chem.* 2006; **44**: 692.
13. (a) Wiggelsworth RD, Raynes WT, Sauer SPA, Oddershede J. *Mol. Phys.* 1997; **92**: 77; (b) Wiggelsworth RD, Raynes WT, Sauer SPA, Oddershede J. *Mol. Phys.* 1998; **94**: 851; (c) Sauer SPA, Møller CK, Koch H, Páidarová I, Špirko V. *Chem. Phys.* 1998; **238**: 385; (d) Wiggelsworth RD, Raynes WT, Kirpekar S, Oddershede J, Sauer SPA. *J. Chem. Phys.* 2000; **112**: 3735; Wiggelsworth RD, Raynes WT, Kirpekar S, Oddershede J, Sauer SPA. *J. Chem. Phys.* 2001; **114**: 9192; (e) Sauer SPA, Raynes WT, Nicholls RA. *J. Chem. Phys.* 2001; **115**: 5994.
14. (a) Kirpekar S, Sauer SPA. *Theor. Chem. Acc.* 1999; **103**: 146; (b) Sauer SPA, Raynes WT. *J. Chem. Phys.* 2000; **113**: 3121; Sauer SPA, Raynes WT. *J. Chem. Phys.* 2001; **114**: 9193; (c) Grayson M, Sauer SPA. *Mol. Phys.* 2000; **98**: 1981; (d) Provasi PF, Aucar GA, Sauer SPA. *Int. J. Mol. Sci.* 2003; **4**: 231; (e) Barone V, Provasi PF, Peralta JE, Snyder JP, Sauer SPA, Contreras RH. *J. Phys. Chem. A* 2003; **107**: 4748.
15. Barone V, Peralta JE, Contreras RH, Sosnin AV, Krivdin LB. *Magn. Reson. Chem.* 2001; **39**: 600.
16. Peralta JE, Contreras RH, Snyder JP. *J. Chem. Soc., Chem. Commun.* 2000; **20**: 2025.
17. Reed AE, Curtiss LA, Weinhold F. *Chem. Rev.* 1988; **88**: 899.
18. Cuevas G, Juaristi E. *J. Am. Chem. Soc.* 2002; **124**: 13088.
19. Bax A, Freeman R, Kampsell SP. *J. Am. Chem. Soc.* 1980; **102**: 4849.
20. Schmidt MW, Baldrige KK, Boatz JA, Elbert ST, Gordon MS, Jensen JH, Koseki S, Matsunaga N, Nguyen KA, Su SJ, Windus TL, Dupuis M, Montgomery JA. *J. Comput. Chem.* 1993; **14**: 1347.
21. Møller C, Plesset MS. *Phys. Rev.* 1934; **46**: 618.
22. Krisnan R, Binkley JS, Seeger R, Pople JA. *J. Chem. Phys.* 1980; **72**: 650.
23. Ågren H, Angeli C, Bak KL, Bakken V, Christiansen O, Cimiraglia R, Coriani S, Dahle P, Dalskov EK, Enevoldsen T, Fernandez B, Haettig C, Hald K, Halkier A, Heiberg H, Helgaker T, Hettema H, Jensen HJA, Jonsson D, Joergensen P, Kirpekar S, Klopper W, Kobayashi R, Koch H, Ligabue A, Lutnaes OB, Mikkelsen KV, Norman P, Olsen J, Packer MJ, Pedersen TB, Rinkevicius Z, Ruddberg E, Ruden TA, Ruud K, Salek P, Sanchez de Meras A, Saue T, Sauer SPA, Schimmelpfennig B, Sylvester-Hvid KO, Taylor PR, Vahtras O, Wilson DJ. *Dalton, A Molecular Electronic Structure Program, Release 2.0.* 2005; see <http://www.kjemi.uio.no/software/dalton/dalton.html>.
24. Sheldrick GM. *SHELXL 97, Program for the Refinement of Crystal Structures.* University of Göttingen: Göttingen, Germany, 1997.